Cell, Vol. 107, 631–641, November 30, 2001, Copyright ©2001 by Cell Press

The Overall Pattern of Cardiac Contraction Depends on a Spatial Gradient of Myosin Regulatory Light Chain Phosphorylation

Julien S. Davis,[1,4] Shahin Hassanzadeh,[1,4] Steve Winitsky,[1] Hua Lin,[1] Colleen Satorius,[1] Ramesh Vemuri,[1,5] Anthony H. Aletras,[2] Han Wen,[2] and Neal D. Epstein[1,3]

[1] Molecular Physiology Section
Cardiology Branch
National Heart, Lung, and Blood Institute
National Institutes of Health
Bethesda, Maryland 20892

[2] Laboratory of Cardiac Energetics
National Heart, Lung, and Blood Institute
National Institutes of Health
Bethesda, Maryland 20892

Summary

Evolution of the human heart has incorporated a variety of successful strategies for motion used throughout the animal kingdom. One such strategy is to add the efficiency of torsion to compression so that blood is wrung, as well as pumped, out of the heart. Models of cardiac torsion have assumed uniform contractile properties of muscle fibers throughout the heart. Here, we show how a spatial gradient of myosin light chain phosphorylation across the heart facilitates torsion by inversely altering tension production and the stretch activation response. To demonstrate the importance of cardiac light chain phosphorylation, we cloned a myosin light chain kinase from a human heart and have identified a gain-in-function mutation in two individuals with cardiac hypertrophy.

Introduction

The efficient contraction of the heart utilizes both a compressing and wringing motion to eject blood from the ventricles. This wringing motion, or torsion, is a striking aspect of the beating heart when viewed in a surgically opened chest. Torsion depends, in part, on the helical orientation of the cardiac myofibers that spiral in a left-handed helix from the tip (apex) to the top (base) of the heart at the epicardial surface. On the inner (endocardial) surface of the ventricles, the fibers have a counter right-handed helical orientation (Streeter et al., 1969; Greenbaum et al., 1981). Our hands mimic these orientations when wringing an object, with the fingers on the left and right hands forming the respective helical directions, and the thumbs denoting the upward spiral. Beyond the increased efficiency provided by torsion, the two distinct helical orientations of the fibers are believed to help equalize stress and strain throughout the heart. Models of this equalization have all assumed uniform mechanical properties of fibers across the heart (Arts et al., 1984; Beyar and Sideman, 1986). It has been previously observed, but not fully understood, that the epicardial fibers dominate the endocardial fibers (Buchalter et al., 1990; Maier et al., 1992; Young et al., 1994). That is, despite the counter-helical orientation of the endocardial fibers, the full thickness of the wall moves with the epicardial twist.

At the molecular level, the contraction of cardiac muscle is driven by isoforms of myosin molecules that hydrolyze ATP, providing energy to move interdigitating thick myosin filaments past actin-containing thin filaments. Myosin heads constitute the crossbridges that extend outward from the thick filament backbones and repetitively bind to, move, and detach from sites on the actin-containing thin filament. The myosin heads taper to an α-helical neck that connects the head to the rod region. The rod is responsible for the self-assembly of the myosin molecules into the thick filaments. The α-helical myosin neck region is supported by two dumbbell-shaped molecules. These molecules are the essential light chains (ELC) and regulatory light chains (RLC). Clusters of mutations throughout the human cardiac myosin head cause hypertrophic cardiomyopathy (Rayment et al., 1995). The myosin head mutations have been used to show that slow skeletal muscle expresses β-cardiac myosin (Cuda et al., 1993). This finding has allowed functional and structural studies of the mutant cardiac myosins from HCM patients to be performed on slow skeletal muscle biopsies from these patients (Cuda et al., 1993; Lankford et al., 1995; Levine et al., 1998).

Phosphorylation of the RLC in smooth muscle and nonmuscle myosins controls the activation of the myosin ATPase (Bresnick, 1999). RLC phosphorylation of skeletal/cardiac muscle myosins, however, has only been shown to produce a modest increase in tension and an increase in Ca^{2+} sensitivity at submaximal levels of Ca^{2+} activation (reviewed by Sweeney et al., 1993). Thus, the major control of tension in these muscles is at the level of the thin filament, through the binding of Ca^{2+} to the troponin-tropomyosin complex. Electrical stimulation increases the level of Ca^{2+} bound to troponin-tropomyosin, allowing actin and myosin to interact and generate force. Recently, we have shown that the tension increase associated with RLC phosphorylation is accompanied by a change in a property called stretch activation (J.D. et al., submitted).

The stretch activation response is an intrinsic property of unknown physiologic significance in most muscles. It is exaggerated in the indirect flight muscle (IFM) of flies and, as such, is responsible for the oscillatory power required for flight. It has been previously conjectured to be important to the vertebrate heart (Pringle, 1978; Steiger, 1977). Indeed, the use of the word "beating" to describe the movement of wings, as well as the heart, reflects the fact that both use oscillatory power. Mutant *Drosophila* expressing a nonphosphorylated myosin RLC in the IFM lose the stretch activation response; although their IFM produces normal isometric tension, their oscillatory power is decreased and these flies are flightless (Tohtong et al., 1995).

[3] Correspondence: nepstein@helix.nih.gov
[4] These authors contributed equally to this work.
[5] Present address: Scientific Review Office, National Institute on Aging, National Institutes of Health, Bethesda, Maryland 20892.

Mutations in both the ELC and RLC cause a rare form of midcavity HCM (Poetter et al., 1996). This variant morphology is characterized by hypertrophied papillary and adjacent ventricular muscle with little or no effect on the apex of the heart. Papillary muscles from transgenic mice expressing a patient's mutant ELC show a dramatic change in the stretch activation response long before they develop any observable hypertrophy (Vemuri et al., 1999). Because the mutant ELC gene is uniformly distributed throughout the ventricles, the pattern of midventricular hypertrophy identifies the parts of the heart that most depend on the stretch activation response. When deprived of it, these parts develop a compensatory hypertrophy. The human mutations surrounding the site of RLC phosphorylation are associated with the same rare midcavity hypertrophy as hearts of patients and mice with the ELC mutation. In contrast to the rare event of a myosin light chain mutation, normal hearts produce a continuous turnover of RLC phosphorylation. Thus, modulation of stretch activation through RLC phosphorylation could have important consequences to normal cardiac physiology.

We now present evidence that the complex muscle mechanics of the beating heart are facilitated by a spatial gradient from high (epicardial) to low (endocardial) levels of phosphorylated myosin RLC that is matched by levels of a myosin light chain kinase (MLCK) we have cloned from human heart. Mechanical studies of single slow muscle fibers show that this spatial gradient of RLC phosphorylation will increase tension, decrease the stretch activation response of the epicardial fibers, and produce the converse effect in the endocardium. The different muscle mechanics across the ventricular wall support cardiac torsion and help explain the pattern of cardiac contraction viewed with magnetic resonance imaging. The importance of this property to cardiac function is highlighted by the report of a gain-in-function MLCK mutation in two individuals with cardiac hypertrophy.

Results

Distribution of Phosphorylated RLC in Heart

In order to study the in vivo effect of phosphorylated cardiac myosin RLC, a polyclonal antibody was raised against a peptide containing the RLC-phosphorylated serine with the three flanking residues on either side. After an initial attempt to raise a useable antibody failed, inoculation with a concatamer of two such peptides produced specific antibodies. Two polyclonals were made, one against human (huRLCP) and another against murine (muRLCP) sequence. On Western blot, both antibodies detected only the phosphorylated human cardiac RLC. The specificity of these antibodies hold for either the expressed RLC alone or the RLC/ELC complex, which is the human ventricular RLC and ELC bound to the human β-myosin heavy chain light chain binding region (aa 778–840) as seen in Figures 1A and 1C. By Western blot analysis, both antibodies detected a background of RLCP in either mouse or human heart that is increased upon the addition of expressed myosin light chain kinase (Figures 1A and 1C). HuRLCP is specific for human substrate, while muRLCP reacts with rabbit, murine, and human substrate (Figures 1A and 1C). Detection by this antibody is reversed by treatment with a serine/threonine phosphatase, PP1 (Upstate), in both fresh-frozen murine cardiac tissue samples and Western blot analysis of phosphorylated expressed human RLC (Figures 1B and 1C).

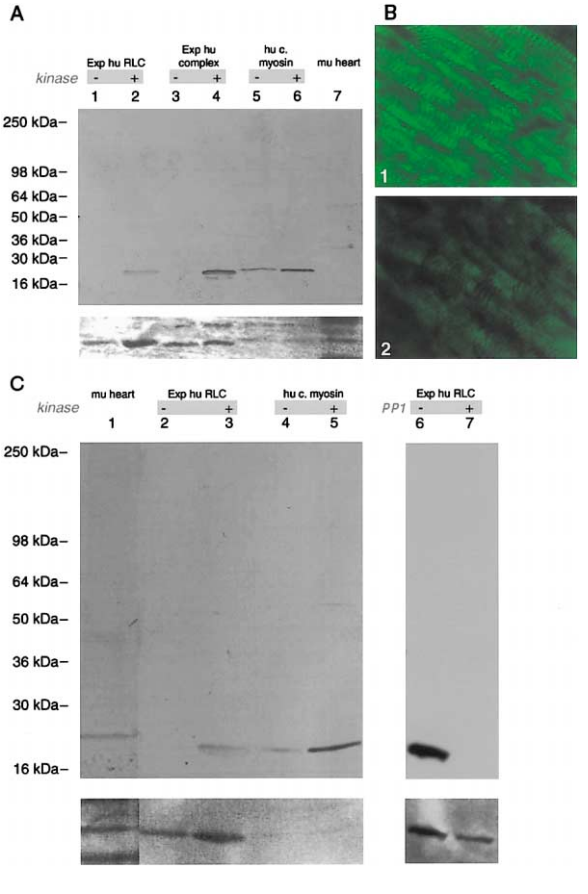

Figure 1. Western Blot Showing Specificities of HuRLCP and MuRLCP Antibodies

(A) Western blot with HuRLCP antibody. Expressed human RLC without (−) (lane 1) and with (+) (lane 2) kinase. RLC/ELC complex (human β-myosin light chain binding region, ELC, and RLC) without (lane 3) and with (lane 4) kinase. Myosin extracted from human heart (lane 5) and with added kinase (lane 6). Mouse heart homogenate (lane 7). Coomassie blue stain of protein loading is shown below each lane.

(B) Fresh-frozen murine heart stained with MuRLCP antibody. Detection of RLCP in thick filaments (B1) is reversed by PP1 phosphatase treatment (B2).

(C) Western blot with MuRLCP antibody. Mouse heart homogenate (lane 1). Expressed human RLC without (lane 2) and with (lane 3) kinase. Extracted human cardiac myosin without (lane 4) and with (lane 5) kinase showing a baseline level of phosphorylation in extracted human cardiac myosin that is increased upon treatment with kinase. Phosphorylated RLC detection (lane 6) is reversed by PP1 phosphatase treatment (lane 7).

When used to stain a sample of normal human cardiac ventricle, both huRLCP (Figure 2A) and muRLCP (data not shown) detect phosphorylated myosin thick filaments. In order to study the global pattern of phosphorylated RLC across the heart, muRLCP was used to stain longitudinal and transverse sections of normal murine

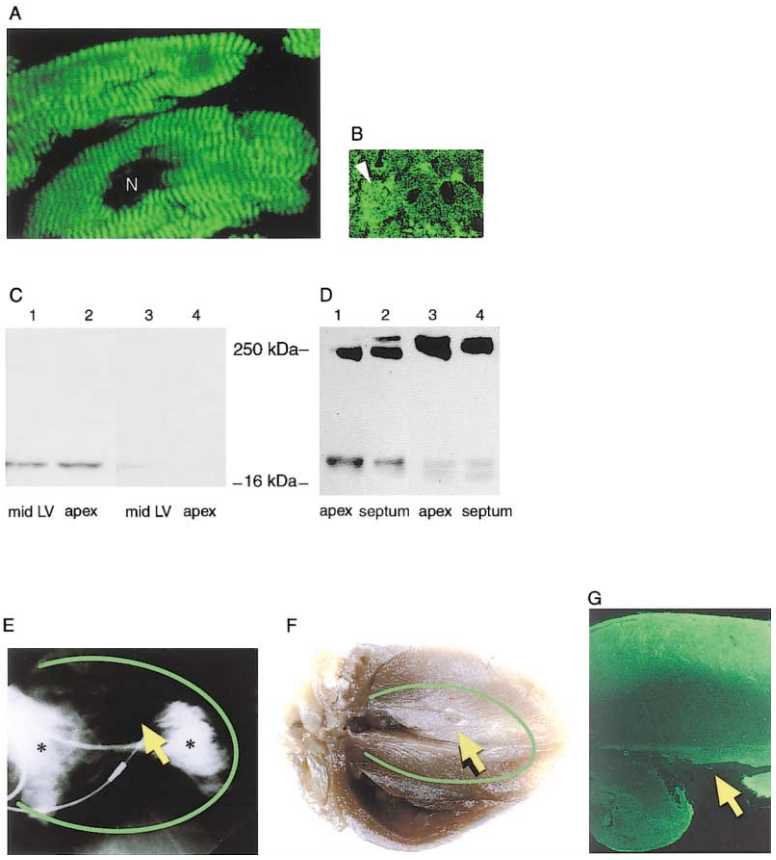

Figure 2. Gradients of RLC Phosphorylation in the Heart

(A) HuRLCP antibody staining of the A bands of two normal human ventricular myocytes. The absence of staining of the central nucleus (N) is evident in the larger cell.

(B) Cross-sections of three fibers (arrow denotes higher level of RLCP) from highly phosphorylated mouse epicardium stained with muRLCP showing the fiber-to-fiber patchy distribution of RLC phosphorylation.

(C) Western blot using huRLCP antibody (lanes 1 and 2) and antibody against total RLC (lanes 3 and 4). A higher ratio of phosphorylated RLC (lane 2) to total RLC (lane 4) is present in the apex of the human heart compared with ratio of phosphorylated RLC (lane 1) to total RLC (lane 3) in mid-left ventricle. Separate gels for lanes 1 and 2 and lanes 3 and 4 were loaded with equal amounts of protein.

(D) Similar study using rabbit heart tissue shows a higher ratio of phosphorylated to total RLC in apex versus septal tissue. High molecular weight bands at top of gel are myosin stained with MF-20 antibody.

(E) Ventriculogram of patient with M149V ELC mutation, showing the constricted hourglass-shaped left ventricular cavity due to hypertrophy of the papillary muscle and adjacent endocardium (yellow arrow). The normally open left ventricular cavity, as pictured in Figure 4C, now excludes dye from the middle of the cavity leaving two cavities marked with an asterisk connected by a stenotic passage. (Adapted from Poetter et al., 1996; reprinted with permission of Nature Publishing Group and Dr. Neil Epstein, Nat. Genet., *13*, 1996, pp 63–69.)

(F) Longitudinal section of transgenic mouse heart expressing human M149V ELC mutation. Hypertrophy of the papillary muscle and adjacent endocardium in the patient's heart is reproduced in this mouse (yellow arrow). (Adapted from Vemuri et al., 1999; reprinted with permission of PNAS and Dr. Neil Epstein, Proc. Natl. Acad. Sci. USA, *96*, 1999, pp 1048–1053.)

(G) A representative normal mouse heart stained with muRLCP antibody demonstrating hypophosphorylated papillary muscle and adjacent endocardium (yellow arrow) that corresponds with the hypertrophied region in transgenic mouse (Figure 2F) and patient heart (Figure 2E).

hearts. A nonuniform but reproducible gradient of expression extends inward from the apex and epicardium (Figures 2G, $4B_3$, and $4B_4$). Western blot analysis with human and rabbit tissue samples from apex and midventricle, stained with muRLCP, confirms this nonuniform pattern of expression across species (Figures 2C and 2D). Within regions of high expression in the heart there is significant fiber-to-fiber variation in RLC phosphorylation (Figure 2B).

Cardiac RLC Phosphorylation Correlates with the Hypertrophic Pattern in Hearts of Patients with RLC and ELC Mutations

The most dramatic aspect of the pattern of RLC phosphorylation in the normal human, mouse, and rabbit hearts is that the region of midcardiac hypertrophy in patients with either light chain mutations or transgenic mice with the ELC mutation (Poetter et al., 1996) matches the pattern of RLC hypophosphorylation in the normal heart. Although human hearts have not been available for detailed in situ studies, the 1-year-old transgenic mice expressing the human mutant ELC reproduce the midcavity hypertrophy phenotype of the patients with the same (M149V) mutant ELC (Vemuri et al., 1999). The midventricular hypertrophy of a patient with the M149V mutation is evident in a ventriculogram (Figure 2E). In transgenic mouse hearts expressing the same mutant ELC (Figure 2F), the dramatic hypertrophy of the papillary muscles and the adjacent endocardium produces the hourglass shape of the left ventricular cavity. The comparison shows that the regions of midcavity hypertrophy in patients and transgenic mice correspond to the hypophosphorylated region in a normal mouse heart (Figure 2G).

The Effect of RLC Phosphorylation on the Kinetics of Contraction and Tension in Rabbit Skeletal Muscle Fibers

Rabbit and human slow skeletal muscle fibers are optimal preparations to study the crossbridge cycle kinetics of cardiac myosin for the following reasons: (1) Human and rabbit slow skeletal muscle fibers express cardiac myosin (Cuda et al., 1993). (2) The small size of cardiac muscle cells, their branching architecture, and their large amount of associated connective tissue make it difficult to obtain reliable mechanical results from single

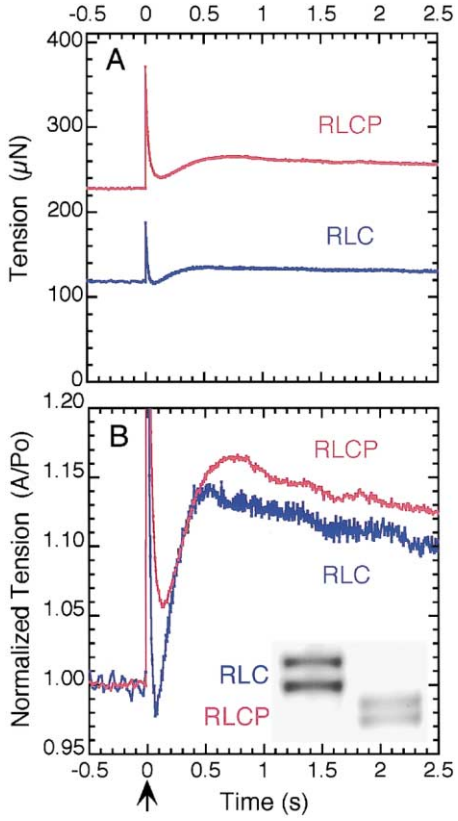

Figure 3. Changes in the Kinetics of Stretch Activation and Fiber Tension due to Regulatory Light Chain Phosphorylation

A Large step-stretch of 12 nm per half sarcomere was applied to a single isometrically contracting fiber at time zero (see arrow). Detergent-skinned rabbit soleus slow type I fibers were used. Sufficient Ca^{2+} was added to the activating solution to produce 20% maximal tension with RLC-containing fibers at 20°C. The inset shows gel analysis of segments of the fiber before and after RLC phosphorylation.

(A) Note the large increase in the baseline isometric tension (before stretch at time zero) from RLC phosphorylation.

(B) The same data as in Figure 3A, but with the transients normalized to their isometric tension in order to highlight changes in the shape caused by RLC phosphorylation. Note the increase in fiber tension from RLC phosphorylation illustrated in Figure 3A is matched here by a reciprocal 41% depression in the delayed rise in tension or stretch activation response.

cardiac cells or ventricular strips. (3) The kinase we cloned from human heart is expressed throughout skeletal muscle. (4) The stretch activation response was noted in skeletal muscle before it was described in the heart.

Therefore, in order to study the effect of RLC phosphorylation on cardiac mechanics, we evaluated slow fibers from rabbit soleus muscle. Single skinned fibers were phosphorylated with expressed human skeletal/cardiac MLCK (see below). Each fiber was subjected to large stretches (0.4%–0.8% muscle lengths) before and after RLC phosphorylation. Figure 3A shows the dramatic ~2-fold increase in isometric tension caused by RLC phosphorylation. Consequently, the magnitude of the tension increase caused by stretch and the ensuing tension transient is noticeably greater in the phosphorylated RLC-containing fibers than in the nonphosphorylated RLC fibers. Changes in the shape of the tension transients also occur with phosphorylation and are best compared in Figure 3B, where they are normalized to their respective isometric tensions. Here, it is evident that the trough-to-peak excursion is proportionally greater in the RLC versus RLCP containing fibers (17% and 10% of normalized isometric tension, respectively). Relaxation kinetics studies that impose small step-stretches on these fibers have shown that the stretch activation response (Huxley-Simmons phase 3) is disproportionately increased in fibers without phosphorylated RLC (J.D. et al., submitted). Thus, in both large- and small-stretch studies, the increased tension produced by RLCP is associated with a reciprocal drop in the stretch activation response while the converse effect occurs in nonphosphorylated fibers. These mechanical differences, associated with the gradient of RLC phosphorylation across the ventricular wall, help explain how cardiac torsion is generated.

Cloning of the Human Skeletal Muscle Myosin Light Chain Kinase from Human Heart

In order to further study the gradient of RLC phosphorylation, we cloned an MLCK (MYLK2) from human heart. Since the first report that cardiac myosin RLC is phosphorylated in vivo (Perrie et al., 1972), there has been an unsuccessful search for the active cardiac kinase(s). Because cardiac β-myosin and its RLC is expressed in slow skeletal muscle fibers of rabbits and humans, the skeletal MLCK has been a candidate kinase. Despite this intuition, the existence of skeletal MLCK in the heart is controversial (Herring et al., 2000). We reasoned that the active sarcomeric myosin light chain kinase in heart, if not actually the skeletal isoform, would likely share homology with the catalytic region of the skeletal muscle MLCK. For RT-PCR, we designed a set of primers from this region of the gene. Fragments of identical sequence that cross an intron-exon boundary were amplified from rabbit heart and skeletal muscle RNA. Degenerate versions of these primers were used to amplify the homologous fragment from human cardiac RNA. The sequence from this fragment was used to generate both 3′- and 5′-RACE products. The gap between the two RACE products was closed by RT-PCR amplification of human cardiac RNA. The full-length cDNA obtained in this way matched the full-length cDNA that we cloned from human skeletal muscle RNA. The human amino acid sequence is 89% homologous to rabbit skeletal MLCK. Most of the discordance is in the first 250 residues, before the start of the catalytic region. A P1 genomic clone containing the full-length human gene was obtained by PCR library screening (Genome Systems) using an intron-based primer pair derived from the original human cardiac RT-PCR fragment. The full-length cardiac MLCK cDNA sequence is embedded in the genomic P1 clone and all 12 intron-exon boundaries have been identified. The P1 clone has been mapped to chromosome 20q13.3.

The Study of the Skeletal/Cardiac MLCK Pattern of Distribution in Skeletal and Cardiac Tissue

In order to study the distribution of the MLCK cloned from human heart, a polyclonal antibody to the entire

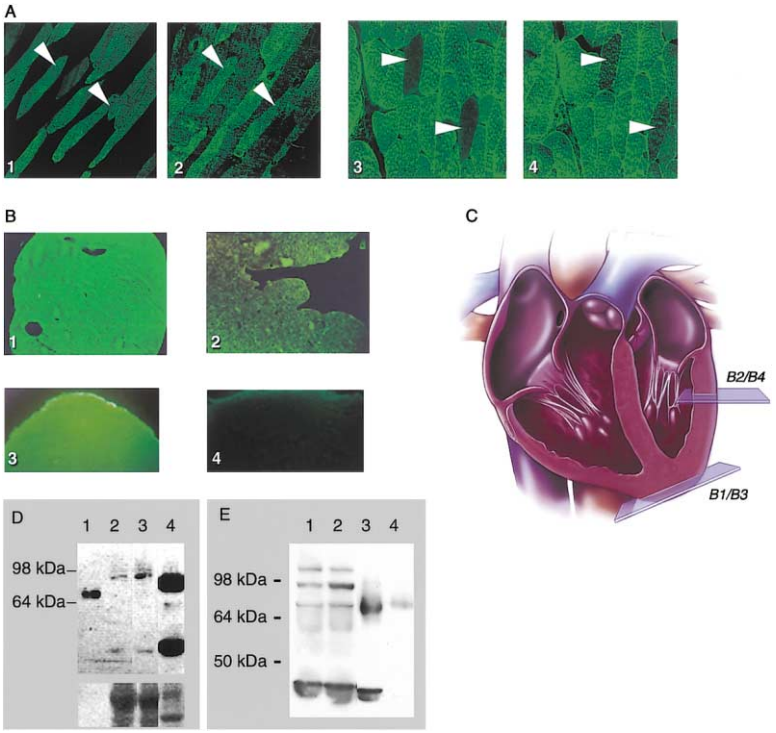

Figure 4. Spatial Distribution of Skeletal/Cardiac MLCK and Phosphorylated RLC

(A) Immunofluorescent staining of serial sections of human deltoid muscle with huRLCP (panel A_1) and antibody against human skeletal/cardiac MLCK (panel A_2), to show colocalization. Parallel studies on serial sections of rabbit skeletal muscle are shown in (panels A_3 and A_4). Arrows mark the same fibers in serial sections.

(B) Immunofluorescent staining of transverse slices from mouse heart shows a gradient of MLCK decreasing from the apex (panel B_1) to the base (panel B_2) of the heart. This mirrors the gradient of phosphorylated RLC (panels B_3 and B_4) stained with muRLCP staining.

(C) Artist's rendition of the heart showing the regions from which the tissue slices in 4B (panels 1–4) were taken.

(D) Western blot detection of MLCK in mouse heart with antibody against the human enzyme. Fragments from mouse heart (lanes 2 and 3) run higher than expressed human MLCK (lane 1). Apical tissue (lane 3) has a higher MLCK signal compared to interventricular septal tissue (lane 2). A mouse skeletal muscle tissue control is presented in (lane 4). Proteolytic bands, common to lanes 2–4, run at low MW. Protein loading using Coomasie blue stain is shown at bottom.

(E) Western blot showing fragments detected by antibody against human MLCK. 74 kDa fragment present in human heart septum (lane 1) and apex (lane 2) matches the fragment corresponding to skeletal muscle MLCK in lane 3 and expressed human skeletal MLCK in (lane 4). Additional bands running at 98 kDa and 120 kDa are present in lanes 1 and 2. There is an increased concentration of the 98 kDa band in apical tissue (lane 2). Protein loading is shown at the bottom with an antibody to GAPDH.

human protein was produced. The full-length cDNA encoding the human MLCK protein, with a 5′-FLAG-tag sequence, was expressed in a baculoviral system (Pharmingen). The FLAG-tag affinity purified protein was used to inoculate rabbits according to standard protocols. The serum from inoculated rabbits was affinity purified against the full-length protein. This antibody detects the expressed human MLCK and the corresponding fragment in Western blots of human and mouse heart or skeletal muscle. Immunofluorescent studies on fresh-frozen samples were also performed.

The MLCK antibody against human skeletal/cardiac myosin lightchain kinase was initially characterized by staining serial fresh-frozen sections of normal human quadriceps tissue. Alternate serial sections probed with huRLCP or anti-MLCK show costaining (Figures $4A_1$ and $4A_2$). Similar findings are seen in rabbit skeletal muscle using the same anti-MLCK antibody paired with the muRLCP antibody (Figures $4C_3$ and $4C_4$).

In order to evaluate the presence and distribution of skeletal/cardiac MLCK in a normal heart, mouse hearts were flash frozen in cooled isopentane immediately following sacrifice. Serial 20 μm thick longitudinal and transverse slices from the apex through the midventricular region were prepared. Samples from a series of normal mice were probed with anti-MLCK antibodies. Immunofluorescent staining consistently showed an increased intensity in the apical cross-sections compared to the midventricular regions (Figures $4B_1$ and $4B_2$). Adjacent serial sections show the correlation with RLCP signals (Figures $4B_3$ and $4B_4$). Western blot analysis of tissue homogenates from mouse septum and apex are consistent with the fluorescent studies (Figure 4D). A sample from apex and septum of a transplanted human heart, frozen soon after harvest, shows a similar distribution (Figure 4E). In the human heart, the skeletal/cardiac MLCK fragment matching the 74 kDa expressed human MLCK is observed along with two larger fragments of 98 and 120 kDa (Figure 4E). These larger fragments may represent additional crossreacting proteins, alternatively spliced isoforms, and/or posttranslational modifications of the 74 kDa fragment. The 98 kDa fragment is consistently of greatest intensity in human apical samples. This may be the source of increased levels of RLCP at the apex.

A Mutant Human Skeletal/Cardiac RLC Kinase with Abnormal Kinetics

We reasoned that since mutations in the RLC substrate of the kinase cause cardiac hypertrophy, MLCK mutations might also be found in a population of patients with cardiac hypertrophy.

Intron-exon boundaries established during the cloning were used to generate intron-based primer pairs for PCR amplification for all 12 exons. The MLCK genes from 490 unrelated patients with cardiac hypertrophy and 189 normal controls were screened. A portion of the gene from 500 coronary artery disease patients was also screened.

Single strand conformation polymorphism (SSCP) de-

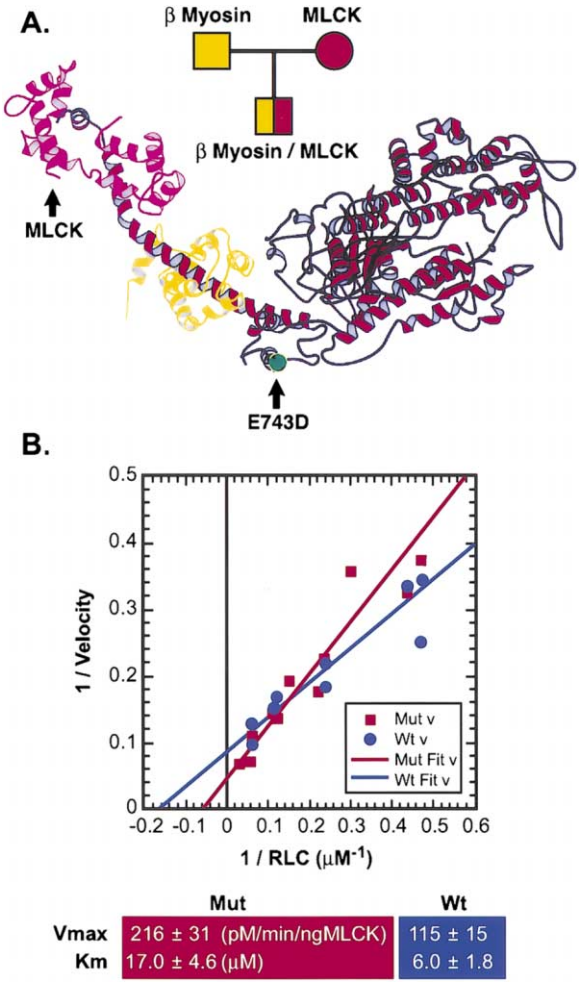

Figure 5. Inheritance, Substrate Site, and Kinetics of the Mutant Human Skeletal/Cardiac MLCK

(A) 3D structure of chicken skeletal muscle myosin S1 showing the homologous site to the inherited human E743D heavy chain mutation on a short α-helix adjacent to the ELC. The approximate position of the MLCK target site (RLC serine 15) is indicated. Inheritance of the mutations is depicted in the pedigree. ELC is in yellow and RLC is in magenta.

(B) Double reciprocal plot showing gain of function in mutant expressed MLCK (red) compared with expressed wild-type (blue) protein. V_{max} and K_m of both proteins are shown below.

tection on gels was used for screening. Although a number of polymorphisms (to be published in a separate article) were observed, only a single mutation was identified. This is a double point mutation inherited on the maternal haplotype by a 13-year-old white male proband with early midventricular hypertrophic cardiomyopathy. The MLCK mutations are A87V and A95E. The proband also inherited an E743D β-myosin mutation from his father. Although the son had significant disease at an early age, the father and mother came to medical attention only after the diagnosis of the son. Echocardiographic evaluation shows that both parents have similarly abnormal asymmetrically thickened hearts. The kindred (Figure 5A), being too small for linkage analysis, suggests that the mutant MLCK may be functionally abnormal, and may consequently stimulate cardiac hypertrophy.

Enzyme Kinetics of the Mutant MLCK

In order to further investigate the effect of the mutant kinase, both full-length wild-type and mutant baculoviral-expressed human skeletal/cardiac MLCK proteins were used to phosphorylate the RLC/ELC complex. Figure 5B shows a double reciprocal plot of 1/v versus 1/[S] comparing the mutant and wild-type MLCK. The mutant MLCK shows a gain in function since the V_{max} of the mutant is almost double that of the wild-type MLCK (216 ± 31 versus 115 ± 15 pmol min^{-1} ng^{-1}, respectively). Although the K_m of the mutant is also significantly greater than the wild-type (17.0 ± 4.6 versus 6.0 ± 1.8 μM, respectively), at physiologic concentrations of light chain (~300 μM), differences in V_{max} dominate the rate of RLC phosphorylation.

Detailed Investigation of Muscle Strain Pattern in the Left Ventricle with Noninvasive Phase-Labeled MRI Techniques (metaDENSE)

We have described a differential pattern of myosin RLC phosphorylation from epicardium to endocardium across the ventricular wall. This, together with the biophysical changes observed in single fiber studies, predicts an effect on the global pattern of cardiac contraction. In order to study the pattern of contraction in the normal human heart, we utilized recent developments in phase-labeled MRI motion tracking that allow detailed mapping of muscle strain and torsion distribution in the left ventricular wall (Aletras and Wen, 2001; Callaghan, 1991). One such technique, metaDENSE, has been optimized to map the displacement field of the human heart at 2.8 mm resolution during a breath-hold of 14 heartbeats, over the entire systolic or diastolic period. The spatial resolution of this technique is sufficient to clearly show changes in the contractile strain and torsion of the muscle across the wall. The left ventricle undergoes torsion around its long axis during systolic contraction; i.e., the apex rotates relative to the base. Recoil occurs in the diastolic period. The direction of torsion is consistent with the helical arrangement of the epicardial muscle fibers but counters the helicity of the endocardial fibers. Therefore, the epicardium is thought to produce the torsion during systole.

High-resolution torsion measurements with metaDENSE showed 50%–70% increase in normalized torsion from the epicardial to endocardial border (H.W., unpublished data). Figure 6B is a color-coded distribution of the rotation of the myocardial wall around the left ventricle (LV) center in a slice of the LV perpendicular to its long axis, about one-fourth the LV length from the apex. This distribution is derived from a set of metaDENSE images that encode the wall motion over the entire systolic period. The blue color indicates that the overall rotation is in the left-handed counter-helical direction of the epicardial fibers. The endocardium is darker in color than the epicardium, indicating an increase in the angle of rotation from the epicardial border to the endocardial border. This phenomenon has also been observed with MR tagging studies at lower spatial resolution (Buchalter et al., 1990; Maier et al., 1992; Young et al., 1994).

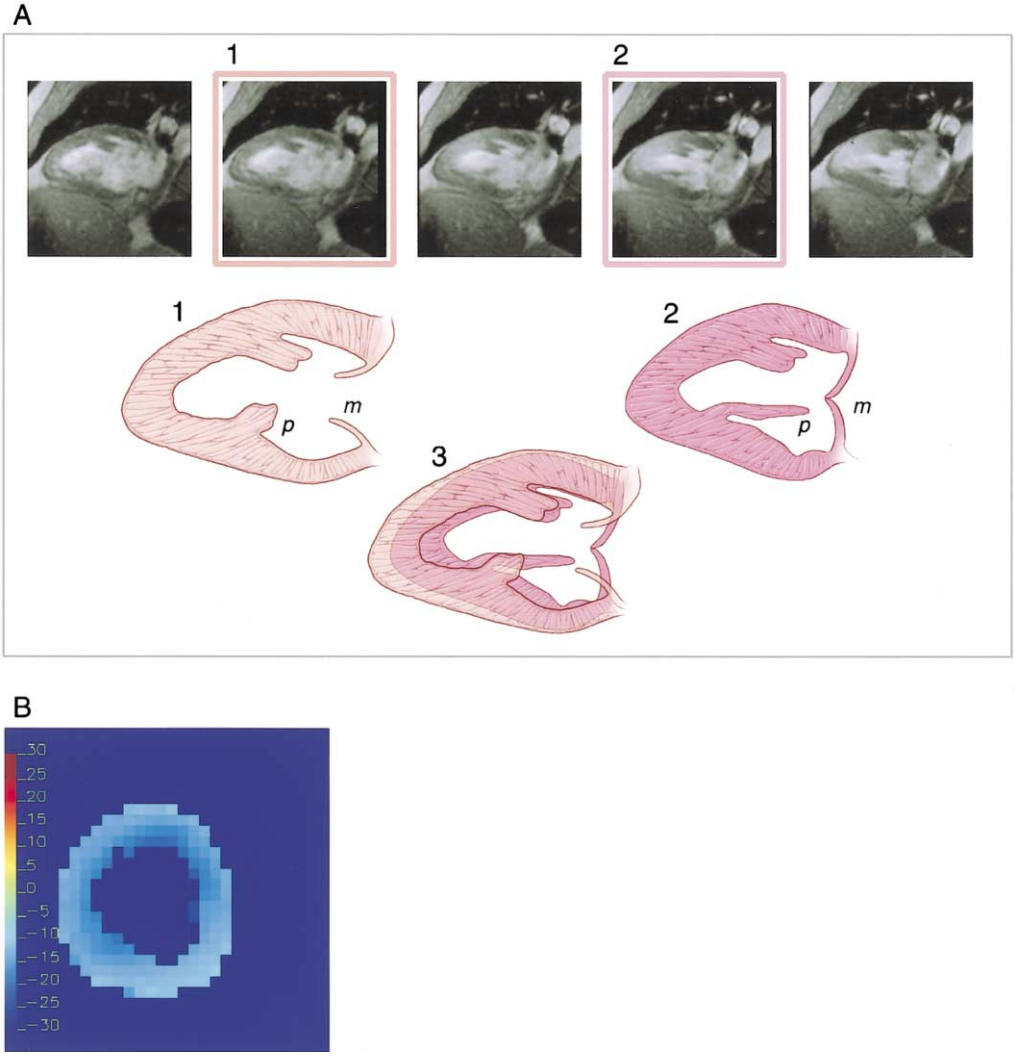

Figure 6. Cine- and Phase-Tagged MRI Images of the Human Heart

(A) Series of cine-MRI images of the left ventricle taken every 50 ms, showing the stretching of the papillary muscles (posterior papillary muscle is marked with a "p" during early systole. Frames 1 and 2 are traced to highlight the papillary muscles, and an overlay (3) provides comparison. The interventricular mitral valve leaflet is labeled with an "m".

(B) A color-coded map of the gradient of angles of rotation, around the LV center. The slice is perpendicular to the left ventricle, at a distance of one-fourth the LV length from the apex. Each square pixel in the map represents ~55 μl of muscle tissue from a volume 2.8 mm × 2.8 mm × 7 mm thick. The color range covers angles from −30° to 30°. The blue appearance indicates that the overall rotation is in the counterclockwise, left-handed helical direction. The darker colors of the endocardium represent higher rotation angles compared to the epicardium.

Changes in Papillary Muscle Anatomy and Movement during Systole Viewed with Cardiac Cine-MRI

In order to study the human cardiac papillary muscles, "cine-MRI" with 50 ms resolution was used to follow their movement throughout systole (Zur et al., 1990). The papillary muscles are among the earliest portions of the ventricle to be electrically stimulated (Rushmer, 1956). A series of five frames (Figure 6A), beginning in cardiac systole, shows that despite the signal to contract, the papillary muscles are stretched early in systole while other portions of the ventricle are contracting. The mechanism, apparent in the five frames, involves the increasing intraventricular pressure in early systole that leads to the closing of the interventricular valves. This in turn stretches the already activated papillary muscles by their valvular attachments, the chordae tendineae (Figure 6A).

Discussion

This report provides evidence for the existence of a spatial gradient of myosin RLC phosphorylation in the heart. We also describe specific changes in the contractile mechanism of slow muscle fibers powered by cardiac β-myosin that occur upon RLC phosphorylation. The differential pattern of phosphorylation and the concomitant variation in the mechanical properties of the

fibers help explain the details of cardiac contraction that are observed with MRI imaging presented here. These findings also help explain why some patients with mutations surrounding the phosphorylatable serine of the RLC have the same rare cardiac phenotype as patients with a distorted stretch activation response associated with a mutant ELC. In order to further investigate the effects of RLC phosphorylation in the heart, we have also cloned an MLCK from human heart. This MLCK is identical to skeletal muscle light chain kinase. Evidence that it is active in the heart comes from two findings. First, we demonstrated that spatial gradients of the MLCK protein correspond to the pattern of RLC phosphorylation. Second, we have identified a gain-in-function mutation in the enzyme found in both a mother and a son with cardiac hypertrophy.

Myosin RLC Phosphorylation Varies from Fiber to Fiber in Skeletal and Cardiac Muscle across Species

We have generated two polyclonal antibodies that recognize the phosphorylated RLC in human, mouse, and rabbit cardiac and skeletal muscle. The studies on skeletal muscle from these three species serve as a control for our studies of RLC phosphorylation in the heart. Beyond the gradient from the outside to the inside of the heart, we have also observed a gradient from apex to the midcardiac region. Within the regions of high levels of phosphorylation, we also observe a patchy pattern of staining that respects fiber boundaries. Thus, RLC phosphorylation levels of tissue homogenates underestimate the high levels and overestimate the low levels of individual fiber RLC phosphorylation. This finding supports the relevance of our studies using fully phosphorylated slow muscle fibers.

Biophysical and Physiologic Consequences of RLC Phosphorylation

Rabbit slow skeletal muscle fibers express cardiac β-myosin. Data obtained from these fibers is thus directly relevant to cardiac myosin function, but avoids a number of problems associated with mechanical studies in cardiac muscle preparations.

RLC phosphorylation causes a very large 2.5-fold increase in fiber tension from 22% to 56% of the maximal Ca^{2+} activated tension of these slow muscle fibers (J.D. et al., submitted). This is one of the largest phosphorylation-induced tension increases ever recorded. Since the contracting heart functions at, and below, half-maximum Ca^{2+}activation, RLC phosphorylation has the potential to modulate cardiac contraction from low tensions to full power at a fixed concentration of Ca^{2+}. Recent small 0.1% step-stretch L-jump experiments show the consequence that RLC phosphorylation has on the kinetics of contraction (J.D. et al., submitted). These kinetic studies demonstrate that the stretch activation response (Huxley-Simmons phase 3) is uniquely affected by RLC phosphorylation. In the large perturbation experiments shown here, phosphorylation-induced changes in the kinetic amplitudes scale in proportion to the size of the stretch applied to the fiber. In 0.8% step-stretch experiments, phosphorylation causes a 41% decrease in the size of the stretch activation peak, a change equivalent to 7% of fiber isometric tension.

We previously observed that an ELC mutation caused the rate of the papillary muscle stretch activation response to become too fast to be matched with the murine physiologic heart rate (Vemuri et al., 1999). Consequently, work produced by this response cannot be used to increase oscillatory power in the portions of the mutant heart that would otherwise be able to take advantage of this property. Here it is shown that RLC phosphorylation leaves the rate unchanged but drops the amplitude of the stretch activation response significantly. This is the possible benefit of maintaining the papillary muscles and endocardium of normal heart in a state of hypophosphorylation, thereby increasing the relative amplitude of the stretch activation response in these parts of the heart. For these reasons, mutations in either light chain burden the papillary muscles and adjacent endocardium by distorting the stretch activation response (either rate or amplitude), leading to a compensatory hypertrophy of these regions. The normally high level of RLC phosphorylation at the cardiac apex could also explain why the apex is not hypertrophied in hearts of patients with mutations in either light chain. That is, the normally hyperphosphorylated apex has a diminished stretch activation response and the distortion of this response by mutations in either light chain is of less consequence to the mechanics of this part of the heart.

The utility of the stretch activation response is apparent from observing the action of papillary muscles in systole (Figure 6A). The papillary muscles tether the interventricular valves that prevent the backflow of blood during cardiac systole. In addition, they also support cardiac torsion by aiding the long-axis shortening of the heart (Rushmer, 1956). Their surgical compromise leads to decreased torsion (Moon et al., 1996) and a low output syndrome (Lillehei et al., 1964). Papillary muscles are the first to be innervated but must continue to contract throughout systole. The delayed pulse of tension, initiated by stretching the activated papillary muscles, is delivered at the end of systole when tension production by these muscles would otherwise be diminishing. The stretch activation response would not be of physiologic importance if its timing did not match heart rate, but in fact, the rate constant of the stretch activation response of rabbit slow muscle fibers is commensurate with the physiologic rate of the rabbit heart (Steiger, 1977; J.D. et al., submitted). This allows for the stretch-induced tension to be added to the force of contraction at the end of systole, much in the same way as a push to a swinging object must be applied at the proper time if oscillatory power is to be increased.

On the other hand, the dramatic increase in slow muscle fiber tension produced by increased RLC phosphorylation of the epicardial fibers enables the hyperphosphorylated epicardial fibers to dominate the right-handed helical twist of the endocardial fibers during the production of torsion. It may also be that the shearing forces that must arise from the counterhelicity of the epicardial and endocardial fibers is minimized by the shape of the stretch activation transient. Because stretching hypophosphorylated fibers triggers an exaggerated drop in tension, the counterhelical force imposed by the hyper-

phosphorylated epicardial fibers on the hypophosphorylated endocardial fibers may produce a reduction in tension of the endocardial fibers. In this way, the shear between epicardial and endocardial fibers would be diminished, producing a corresponding drop in energy/oxygen requirements. This model provides a rationale for the evolutionary conservation of counterhelically oriented fibers in the endocardium and epicardium of vertebrate hearts. It may also contribute to the faster angular velocity of the endocardial fibers as they drop their resistance following a stretch (Figure 6B). In this context, the stretch activation response can also be thought of as a mechanism to return, with an appropriate time delay, some of the tension that is lost in the hypophosphorylated papillary muscles and endocardium.

The Cloning of a Cardiac MLCK

If, in fact, RLC phosphorylation has the important cardiac function presented here, we reasoned that there may be cardiomyopathic patients who have developed disease as the result of an inherited abnormality in the responsible kinase. To date, the existence of a striated myosin RLC kinase in the heart is controversial. Our strategy for cloning such a kinase was based on the similarity between skeletal and cardiac RLC. The distribution of skeletal/cardiac MLCK in mouse and human heart matches the pattern of RLC phosphorylation. This uneven distribution of the MLCK is probably the reason that others have failed to detect the skeletal muscle MLCK in heart (Herring et al., 2000), since homogenates from total heart will contain much less kinase than homogenates from the epicardium and apex.

In the mouse and human heart, the antibody raised against this expressed human skeletal/cardiac MLCK detects two additional larger fragments of 120 kDa and 98 kDa, as well as the unique 74 kDa MLCK fragment seen in human skeletal muscle. Because these additional bands are absent in skeletal muscle, they may represent additional gene products, alternatively spliced isoforms, or posttranslational modifications of the 74 kDa fragment. The increased density of the 98 kDa fragment at the apex may cause increased RLC phosphorylation at that site.

We scanned the DNA of 490 patients with hypertrophic hearts, 189 controls, and 500 patients with coronary artery disease for mutations in the coding portion of the gene. Only a single mutation was found. The V_{max} of the expressed mutant MLCK is double that of expressed wild-type. Although the K_m of the mutant MLCK tripled, this change is probably irrelevant since the physiologic concentration of RLC in muscle is 20-fold greater than the highest K_m. The development of compensatory hypertrophy in the face of a doubling of the V_{max} of the mutant MLCK suggests that a proper balance of RLC phosphorylation is required for proper cardiac function. Both mother and father have asymmetrically hypertrophied ventricles. The son, who has also inherited both his mother's mutant MLCK and his father's mutant β-myosin heavy chain mutation (E743D), had an early midcavity type distribution of hypertrophy at age 13. The increased severity at this young age suggests a compound effect. Figure 5A shows that as a result of his co-inheritance, he has abnormalities at both ends of the myosin neck. Although a sample of two is too small for statistical significance, our ongoing studies on individuals with alleles of the MLCK gene should provide the numbers of individuals needed for such a study.

Conclusions

The work presented here is an example of how variations at a molecular level can be projected through cellular organization to the level of global cardiac function. We have: (1) demonstrated a gradient of myosin RLC phosphorylation across the heart, (2) identified a kinase contributing to the gradient, (3) demonstrated the biophysical consequences of this phosphorylation, and (4) suggested how the gradient of phosphorylation can facilitate an overall pattern of cardiac contraction viewed with MRI imaging.

Experimental Procedures

Subjects

In vivo MR cardiac scans of normal human subjects were conducted on a General Electric 1.5 tesla cardiac scanner. Informed consent for the MRI studies and the genetic screening was obtained in accordance with study protocols 97-H-0026 and 87-H-57, respectively, approved by the Institutional Review Board of the National Heart, Lung, and Blood Institute.

Animal Studies

Animal studies were conducted under protocols 8CB3R and 9CB2 in accordance with the National Heart, Lung, and Blood Institute Animal Care and Use Committee.

Cloning of the Human Skeletal/Cardiac MLCK

The rabbit skeletal muscle MLCK cDNA sequence (Herring et al., 1990) was used to design a set of primer pairs to amplify unique RNA fragments from both rabbit skeletal and cardiac muscle. Product from one pair of primers (upstream 5′-TGATCCAGCTGTACGCAGCC-3′, downstream 5′-CTTGAGGTCCAGGTGCAGC-3′) yielded identically sized 201 bp fragments from both templates. The degenerate downstream primer used to amplify a homologous fragment from human cardiac RNA was 5′-AGGTCCAg/aGTGCAGc/a/t/gACCCg/tCA-3′. The upstream primer, which is highly conserved in rat and rabbit, was not made degenerate: (5′-CATGAACCAGCTTAACCACCG-3′). These primers yielded a fragment of human genomic DNA containing parts of exon 6 and 7 separated by an 81 bp intron. In order to obtain full-length human genomic sequence, a primer based in human intron 6 (5′-CCACGGCTTGCTCCGTGCCT-3′) was used together with an upstream exon 6 primer (5′-ATCGAGACTCCGCATGAGAT-3′) to screen a human P1 library (Genome Systems).

In order to obtain a full-length cDNA from human heart, 5′- and 3′-RACE was performed using a Marathon RACE kit (Clontech). 3′-RACE was initiated with an exon 7-based primer: 5′-TCGAGACT CCGCATGAGAT-3′. An approximately 1100 bp fragment was obtained. 5′-RACE was performed using an exon 6-based primer: 5′-ATCTCATGCGGAGTCTCGA-3′. Indeterminate product was amplified using a seminested exon 3 primer derived from the genomic clone and yielded an 850 bp fragment. The seminested primer is: 5′-TCTGAGGGAACAGCCTGGAAC-3′. The gap between the 5′- and 3′-RACE products was bridged by RT-PCR, amplifying from human cardiac RNA. Each exon was then subsequently located in the genomic P1 clone that had been obtained by selecting with the intron 6-based fragment described above.

MLCK Expression

The whole MLCK cDNA was subcloned into a pVL1393 baculovirus transfer vector (PharMingen) under the polyhedrin promoter with a FLAG-tag at the 5′ end of MLCK. The baculovirus-containing MLCK gene was then constructed with the BaculoGold system (PharMigen) from the transfer vector. The MLCK protein was expressed by infecting the virus into the SF9 insect cells and purified using anti-FLAG affinity agarose resin (Sigma). The purified MLCK was dialyzed

into a buffer containing 10 mM MOPS, 0.5 mM EGTA, 0.2 M NaCl, 1 mM dithiothreitol (DTT), and 10% glycerol, at pH 7.0.

MLCK Kinetics Assay

The phosphorylation of myosin RLC was performed in buffer pH 7.2 containing 50 mM MOPS, 10 mM Mg acetate, 1 mM DTT, 0.6 mM $CaCl_2$, 2×10^{-7} M calmodulin, and 0.5 mM ATP (with ^{32}P-labeled ATP, 30 ci mmol^{-1}) at 25°C. The final MLCK concentration was 28 ng ml^{-1}. The reaction mixture with RLC but without MLCK was preincubated at 25°C for 10 min. The reaction phosphorylation was initiated by the addition of MLCK. Twenty μl aliquots of the reaction mixture were spotted onto Whatman #3 filter paper, and the reaction was stopped by immersing the filter paper in a solution of 10% TCA and 8% sodium pyrophosphate at 4°C. The filter paper was then rinsed three times in a 10% TCA and 2% sodium pyrophosphate solution, once in ethanol, and three times in ether before being air dried. The concentration of phosphorylated RLC labeled with ^{32}P on the filter paper was determined in a scintillation counter.

Myosin Light Chains Complex Expression

Human β-myosin binding domain for the myosin light chains (aa 778–840) was subcloned into a pVL1393 baculovirus transfer vector under the polyhedrin promoter with a FLAG-tag at its 3′ end. Myosin ELC and RLC cDNA sequences were also subcloned into pVL1393 transfer vectors. All three proteins were expressed simultaneously in the baculovirus system by infecting SF9 insect cells with the viruses. Expressed myosin ELC and RLC and the myosin heavy chain binding domain formed a complex that was purified on an anti-FLAG affinity agarose resin (Sigma).

Production of MLCK Antibody

Rabbits were inoculated with the FLAG-tag affinity-purified MLCK protein and boosted at 2, 4, and 6 weeks. The 8- and 10-week sera were affinity purified against the full-length MLCK protein by column chromatography.

L-Jump Experiments

Experimental details and methods of analysis are described in detail elsewhere (Davis, 2000; J.D. et al., submitted).

RLC Phosphorylation Assay

Single fiber segments were assayed to determine the level of RLC phosphorylation by selective extraction of the light chain (Craig et al., 1987) followed by separation of the RLC species by glycerol-PAGE (Perrie and Perry, 1970). The gels were silver-stained and scanned for quantitation.

Enzyme Kinetics

Steady-state kinetic parameters for the mutant and normal myosin light chain kinases were determined by using the nonlinear form of the Michaelis-Menten equation to fit K_m and V_{max} values to initial rate data using the nonlinear least squares fitting routine of the program Kaleidagraph (Synergy Software; Reading, PA).

Acknowledgments

We would like to thank specific individuals for their help: Robert Adelstein and James Sellers for their helpful discussions and careful reading of the manuscript; James Sellers kindly supplied the calmodulin. Fei Wang helped with the baculoviral expression system, and Kazuyo Takeda and Zu-Xi Yu performed the confocal microscopy. Julio Panza and Vandana Sachdev reviewed the echocardiographs. Don Bliss and Martha Blalock helped with figure preparation.

Received April 4, 2001; revised August 29, 2001.

References

Aletras, A.H., and Wen, H. (2001). Mixed echo train acquisition displacement encoding with stimulate echoes: an optimized DENSE method for in-vivo functional imaging of the human heart. Magn. Reson. In Med. *46*, 523–534.

Arts, T., Meerbaum, S., Reneman, R.S., and Corday, E. (1984). Torsion of the left ventricle during the ejection phase in the intact dog. Cardiovasc. Res. *18*, 183–193.

Beyar, R., and Sideman, S. (1986). The dynamic twisting of the left ventricle: a computer study. Ann. Biomed. Eng. *14*, 547–562.

Bresnick, A.R. (1999). Molecular mechanisms of nonmuscle myosin-II regulation. Curr. Opin. Cell Biol. *11*, 26–33.

Buchalter, M.B., Weiss, J.L., Rogers, W.J., Zerhouni, E.A., Weisfeldt, M.L., Beyar, R., and Shapiro, E.P. (1990). Noninvasive quantification of left ventricular rotational deformation in normal humans using magnetic resonance imaging myocardial tagging. Circulation *81*, 1236–1244.

Callaghan. P.T. (1991). Principles of Nuclear Magnetic Resonance Microscopy, First Edition (Oxford: Clarendon Press).

Craig, R., Padron, R., and Kendrick, J.J. (1987). Structural changes accompanying phosphorylation of tarantula muscle myosin filaments. J. Cell Biol. *105*, 1319–1327.

Cuda, G., Fananapazir, L., Zhu, W.S., Sellers, J.R., and Epstein, N.D. (1993). Skeletal muscle expression and abnormal function of beta-myosin in hypertrophic cardiomyopathy. J. Clin. Invest. *91*, 2861–2865.

Davis, J.S. (2000). Kinetic analysis of dynamics of muscle function. Methods Enzymol. *321*, 23–37.

Greenbaum, R.A., Ho, S.Y., Gibson, D.G., Becker, A.E., and Anderson, R.H. (1981). Left ventricular fibre architecture in man. Br. Heart J. *45*, 248–263.

Herring, B.P., Stull, J.T., and Gallagher, P.J. (1990). Domain characterization of rabbit skeletal muscle myosin light chain kinase. J. Biol. Chem. *265*, 1724–1730.

Herring, B.P., Dixon, S., and Gallagher, P.J. (2000). Smooth muscle myosin light chain kinase expression in cardiac and skeletal muscle. Am. J. Physiol. Cell Physiol. *279*, C1656–1664.

Lankford, E.B., Epstein, N.D., Fananapazir, L., and Sweeney, H.L. (1995). Abnormal contractile properties of muscle fibers expressing beta-myosin heavy chain gene mutations in patients with hypertrophic cardiomyopathy. J. Clin. Invest. *95*, 1409–1414.

Levine, R.J., Yang, Z., Epstein, N.D., Fananapazir, L., Stull, J.T., and Sweeney, H.L. (1998). Structural and functional responses of mammalian thick filaments to alterations in myosin regulatory light chains. J. Struct. Biol. *122*, 149–161.

Lillehei, C.W., Levy, M.J., and Bonnabeau, R.C. (1964). Mitral valve replacement with preservation of papillary muscles and chordae tendineae. J. Thorac. Cardiovasc. Surg. *47*, 532–543.

Maier, S.E., Fischer, S.E., McKinnon, G.C., Hess, O.M., Krayenbuehl, H.P., and Boesiger, P. (1992). Evaluation of left ventricular segmental wall motion in hypertrophic cardiomyopathy with myocardial tagging. Circulation *86*, 1919–1928.

Moon, M.R., DeAnda, A., Daughters, G.T., Ingels, N.B., and Miller, D.C. (1996). Effects of chordal disruption on regional left ventricular torsional deformation. Circulation *94*, II143–151.

Perrie, W.T., and Perry, S.V. (1970). An electrophoretic study of the low-molecular-weight components of myosin. Biochem. J. *119*, 31–38.

Perrie, W.T., Smillie, L.B., and Perry, S.V. (1972). A phosphorylated light-chain component of myosin. Biochem. J. *128*, 105P–106P.

Poetter, K., Jiang, H., Hassanzadeh, S., Master, S.R., Chang, A., Dalakas, M.C., Rayment, I., Sellers, J.R., Fananapazir, L., and Epstein, N.D. (1996). Mutations in either the essential or regulatory light chains of myosin are associated with a rare myopathy in human heart and skeletal muscle. Nat. Genet. *13*, 63–69.

Pringle, J.W.S. (1978). Stretch activation of muscle, function and mechanism. Proc. R. Soc. Lond. B Biol. Sci. *201*, 107–130.

Rayment, I., Holden, H.M., Sellers, J.R., Fananapazir, L., and Epstein, N.D. (1995). Structural interpretation of the mutations in the beta-cardiac myosin that have been implicated in familial hypertrophic cardiomyopathy. Proc. Natl. Acad. Sci. USA *92*, 3864–3868.

Rushmer, R.F. (1956). Initial phase of ventricular systole: asynchronous contraction. Am. J. Physiol. *184*, 188–194.

Steiger, G.J. (1977). Stretch activation and tension transients in car-

diac, skeletal and insect flight muscle. In Insect Flight Muscle, R.T. Treager, ed. (Amsterdam: North-Holland), pp. 221–268.

Streeter, D.D., Spotnitz, H.M., Patel, D.P., Ross, J., and Sonnenblick, E.H. (1969). Fiber orientation in the canine left ventricle during diastole and systole. Circ. Res. *24*, 339–347.

Sweeney, H.L., Bowman, B.F., and Stull, J.T. (1993). Myosin light chain phosphorylation in vertebrate striated muscle: regulation and function. Am. J. Physiol. *264*, C1085–1095.

Tohtong, R., Yamashita, H., Graham, M., Haeberle, J., Simcox, A., and Maughan, D. (1995). Impairment of muscle function caused by mutations of phosphorylation sites in myosin regulatory light chain. Nature *374*, 650–653.

Vemuri, R., Lankford, E.B., Poetter, K., Hassanzadeh, S., Takeda, K., Yu, Z.X., Ferrans, V.J., and Epstein, N.D. (1999). The stretch activation response may be critical to the proper functioning of the mammalian heart. Proc. Natl. Acad. Sci. USA *96*, 1048–1053.

Zur, Y., Wood, M.L., and Neuringer, L.J. (1990). Motion-insensitive, steady-state free precession imaging. Magn. Reson. Med. *16*, 444–459.

Young, A.A., Kramer, C.M., Ferrari, V.A., Axel, L., and Reichek, N. (1994). Three-dimensional left ventricular deformation in hypertrophic cardiomyopathy. Circulation *90*, 854–867.

Accession Numbers

The gene for human skeletal/cardiac MLCK has been designated MYLK2. The complete coding sequence for the 596 amino acid residues has been deposited at GenBank (accession number AF325549) (see Experimental Procedures section for details of cloning).